Res Chem Intermed
DOI 10.1007/s11164-015-1992-7

Active carbon-supported nickel–palladium catalysts for hydrodechlorination of 1,2-dichloroethane and 1,1,2-trichloroethene

I. I. Kamińska[1] · **A. Śrębowata**[1]

Received: 27 October 2014 / Accepted: 26 February 2015

Abstract Norit active carbon-supported Ni–Pd catalysts were prepared, by incipient wetness impregnation, from the metal chlorides $NiCl_2 \cdot 6H_2O$ and $PdCl_2$. The catalysts were characterized by temperature-programmed reduction, X-ray diffraction, and scanning electron microscopy, and by temperature-programmed hydrogenation (TPH) of the catalysts after use. When the catalysts were used for gas-phase hydrodechlorination (HDC) of 1,2-dichloroethane (1,2-DCA) and 1,1,2-trichloroethene (TCE), very high activity and stability at a relatively low reaction temperature (503 K) were observed. Hydrodechlorination of TCE led to formation of hydrocarbons as the main products. Use of Ni and Ni–Pd catalysts for hydrodechlorination of 1,2-DCA resulted in very high ($\sim$100 %) selectivity for ethene. TPH of the catalysts after use for HDC of 1,2-DCA and TCE revealed the presence of carbon and chlorine-containing deposits on the surfaces of the catalysts. Formation of the NiC_x fcc phase and the Ni_3C hcp carbide phase were detected for the monometallic nickel and Ni95Pd05 catalysts.

Keywords Ni–Pd catalysts · Active carbon · 1,2-Dichloroethane · 1,1,2-Trichloroethene · Hydrodechlorination

Introduction

The continuous development of industry results in large amounts of harmful substances in the atmosphere, water, and soil. Particular attention should be focused on the chlorinated hydrocarbons, e.g. 1,2-dichloroethane (1,2-DCA) and 1,1,2-trichloroethene (TCE)—substances commonly used in industry as solvents, extractants, and degreasing

✉ A. Śrębowata
asrebowata@ichf.edu.pl

[1] Institute of Physical Chemistry, Polish Academy of Sciences, ul. Kasprzaka 44/52, 01224 Warsaw, Poland

Published online: 07 March 2015

agents. Because of their potential carcinogenic, mutagenic, and teratogenic effects on living organisms, the danger is very serious [1–3]. Therefore, finding effective and inexpensive methods for removal of these compounds is extremely important. One such method is hydrodechlorination (HDC). Noble metals, for example palladium and platinum are effective catalysts of HDC [4–6], but their high cost limits practical application. Nickel, an inexpensive metal with very good catalytic properties in the transformation of chlorinated compounds into value added products, can be an attractive alternative for Pd and Pt [7–20]. Depending on the type of the support different product distributions are obtained. Application of supports with acidic properties, for example the acidic form of BEA zeolite or γ-Al_2O_3, usually leads to formation of vinyl chloride as the main product of HDC of 1,2-DCA [15, 16]; TCE conversion usually leads to hydrocarbons [20].

Microporous Sibunit carbon-supported Ni has proved to be an active, stable and selective catalyst for conversion of 1,2-DCA to ethylene in the presence of hydrogen at low reaction temperatures (503 K) [21].

The purpose of this study was to investigate the effect of addition of small amounts of palladium on the catalytic behavior of Norit CNR 115 carbon-supported nickel in HDC of 1,2-DCA and TCE, and the effect of nickel carbiding, and of fcc NiC_x phase and hcp Ni_3C phase formation, on the properties of Ni–Pd systems. Use of carbon obtained from a renewable raw material by use of a patented version of the phosphoric acid process also has environmental advantages.

Materials and methods

Ni–Pd catalysts supported on active carbon

A commercial activated carbon, CNR115, produced from a renewable raw material by use of a patented version of the phosphoric acid process [22] and supplied by Norit, was used as support. Before preparation of the catalysts the carbon was washed with redistilled water, only, and dried in an air at 393 K.

A series of nickel–palladium catalysts was prepared by incipient wetness co-impregnation of active carbon with aqueous solutions of metal chlorides ($PdCl_2$ and $NiCl_2{\cdot}6H_2O$, both of analytical purity from POCh, Gliwice, Poland). The metal-containing solution was added to an amount of support with the same total pore volume as the volume of solution added. For each catalyst the nickel loading was 5 wt% whereas the amounts of palladium were to furnish the specific atomic percentages listed in Table 1. After impregnation, the catalyst precursors were dried for 24 h with an infrared lamp then mixed by rotary motion of a beaker containing the precursor.

Catalyst characterization and tests of catalytic activity

Temperature-programmed reduction (TPR) of catalyst precursors ($\sim$180 mg) was performed by use of a glass-flow system equipped with a Glow-Mac thermal conductivity detector (TCD). TPR runs were performed in 10 % H_2–Ar at a flow rate of 25 cm^3 min^{-1}; the temperature was ramped from 253 to 823 K at

Table 1 Notation used for Ni, Ni–Pd, and Pd catalysts supported on Norit CNR115

Catalyst notation[a]	Ni100	Ni95Pd05	Ni90Pd10	Ni85Pd15	Pd100
Metal content (wt%)					
Ni	5.00	5.00	5.00	5.00	–
Pd	–	0.45	0.95	1.50	1.50

[a] In catalysts notation Ni*X*Pd*Y* means atomic percentages of nickel and palladium in supported metal phase

10 K min^{-1}. For calibration, known amounts of hydrogen were injected into the hydrogen–argon flow (before and after each TPR run).

Hydrodechlorination of 1,2-DCA and TCE was performed in a glass-flow system equipped with fritted disk on which the catalyst was placed. Before the reactions the catalysts were dried in flowing Ar at 393 K for 0.5 h and reduced in flowing 10 % H_2–Ar at 673 K for 3 h. After reduction, the catalysts were cooled to 503 K and then placed in contact with the reaction mixture (flow of hydrogen + argon + DCA or TCE 42 cm^3 min^{-1}; partial pressure ratios $P_{H2}/P_{C2H4Cl2}$ and $P_{H2}/P_{C2H3Cl3}$ 1:1 and 3:1, respectively).

X-ray diffraction (XRD) experiments were performed with a standard Rigaku Denki diffractometer using Ni-filtered Cu-Kα radiation. Samples before and after HDC of 1,2-DCA and TCE were scanned by a step-by-step technique, at 2θ intervals of 0.04°.

Scanning electron microscopy (SEM) was performed by use of Nova NanoSEM NPE190 equipment operated at an acceleration voltage between 3 and 15 keV.

After reaction with 1,2-DCA and TCE the catalysts were investigated by temperature-programmed hydrogenation (TPH). Progress of TPH runs, using 10 % H_2–He at a flow rate of 25 cm^3 min^{-1} and ramping at 10 K min^{-1}, was followed by mass spectrometry (MA200, Dycor-Ametek, Pittsburgh, USA). Twelve masses were monitored during the experiment, but the major changes were observed at *m*/*z* 28 and 29 (C_2H_x release), and *m*/*z* 36 and 38 (HCl liberation) only.

Results and discussion

Temperature-programmed reduction

The TPR profiles (Fig. 1) showed that complete reduction of Norit CNR115-supported Ni–Pd precursors occurs at <740 K. It can be assumed that the pretreatment conditions before testing of the catalysts (10 % H_2–Ar, 3 h at 673 K) are sufficient for complete reduction of the nickel and palladium precursors to the metals. The temperatures of maximum reduction of $PdCl_2$ and $NiCl_2$ are approximately 500 and 712 K, respectively. The TPR profiles for the bimetallic precursors contain two noticeable reduction maxima, those of the palladium precursor (lower temperature) and nickel precursor (higher temperature). Distinct and well separated peaks suggest that interaction between the Ni and Pd precursors is insignificant. A slight effect of alloying can be observed for Ni95Pd05, for which the temperature difference between

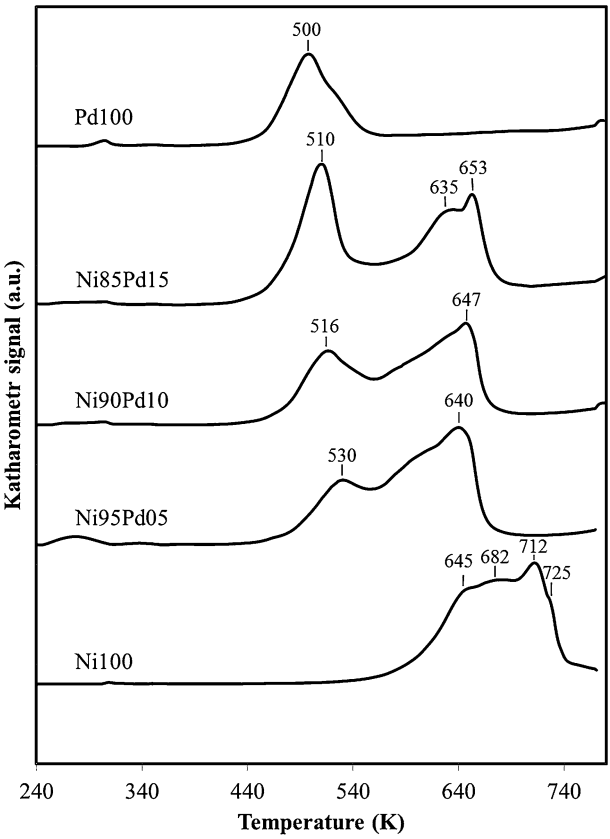

Fig. 1 Temperature programmed reduction (TPR) profiles of Norit CNR115-supported Pd–Ni catalysts

the reduction peaks of the nickel and palladium precursors is the least (110 K). Simagina et al. [10] reported that even the most sophisticated methods used for preparation of Ni–Pd catalysts do not guarantee preparation of homogeneous products. The shift of maximum reducibility from 712 K (for $NiCl_2$) to 640–653 K (for the bimetallic precursors) might indicate that addition of palladium minimizes the temperature of reduction of the nickel precursor. This can be explained by the presence of dissociated hydrogen at pre-reduced palladium centers [10]. A similar effect is very well known for Ni–Pd/Al_2O_3 catalysts [23–25].

Hydrodechlorination of 1,2-dichloroethane and 1,1,2-trichloroethene

Figure 2 shows conversion as a function of time on stream (TOS) for HDC of 1,2-DCA over Pd–Ni catalysts. The monometallic nickel catalyst had negligible activity. Addition of palladium substantially increased the catalytic activity. The highest conversion was obtained for Ni85Pd15 catalyst. Ethene was the desired product of the reaction. Figure 3 shows the changes of selectivity for C_2H_4 during

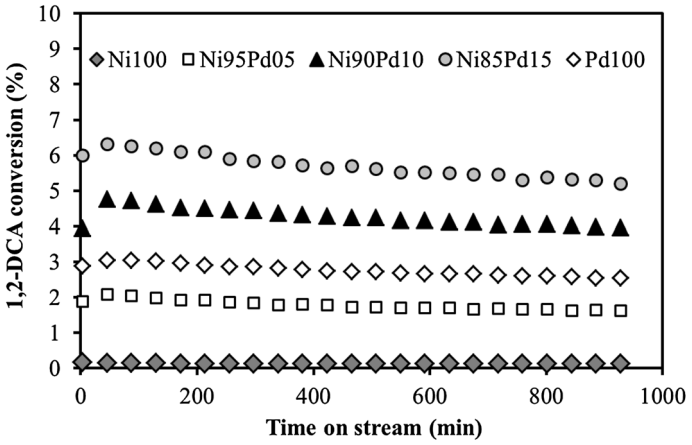

Fig. 2 Changes of conversion as a function of time on stream for hydrodechlorination of 1,2-dichloroethane over Pd–Ni catalysts

HDC of 1,2-DCA. According to earlier studies [21, 26], almost 100 % selectivity for ethene was observed for Ni and Ni–Pd catalysts whereas 65 % selectivity to ethene was observed for palladium as catalyst. This phenomenon is unparalleled in the scientific literature. The excellent hydrogenation activity of palladium usually leads to formation of saturated hydrocarbons as the main reaction products [26–28]. To the best of our knowledge, hydrodechlorination of 1,2-DCA on palladium catalysts usually leads to the formation of ethane as the main product. Thus, the 66 % selectivity for ethene obtained with Pd100 was unexpected. The reason for this uncommon catalytic behavior of palladium could be the specific properties of the Norit support. Mercury porosimetry and SEM studies have shown that Norit CNR115 has a highly developed porous structure which consists of large macropores of diameter between 2 and 30 μm, mesopores of diameter between 10 and 40 nm, and a total pore volume of approximately 1.11 $cm^3\ g^{-1}$. Careful analysis of Norit active carbon has also revealed the presence of substantial numbers of micropores and a specific surface area of 1863 $m^2\ g^{-1}$. These specific properties of Norit carbon probably promote excellent dispersion palladium species. Because it has been found that the dispersion of the metallic active phase can affect both activity and product distribution [29, 30], it is possible that very high dispersion of palladium species on the carbon support (Table 2) is involved in formation of ethene as the main product.

In HDC of TCE the catalysts resulted in substantially higher conversion (Fig. 4) than during HDC of 1,2-DCA (Fig. 3). Negligible activity was observed for the monometallic nickel catalyst (Fig. 4). However, addition of palladium to the nickel catalyst led to a substantial increase of conversion (from 0.3 % for Ni100 to ~50 % for Ni85Pd15 and Pd100) at a rather low reaction temperature (503 K). The synergistic effect was noticed for Ni85Pd15. The main products of HDC of TCE were hydrocarbons, for example C_2H_4, C_2H_6, and C_3H_6 (Table 3). In previous studies [31–33], the largest amounts of ethene were obtained by use of Ni85Pd15 (35 %) and Pd100 (60 %), the catalysts with the maximum Pd loading.

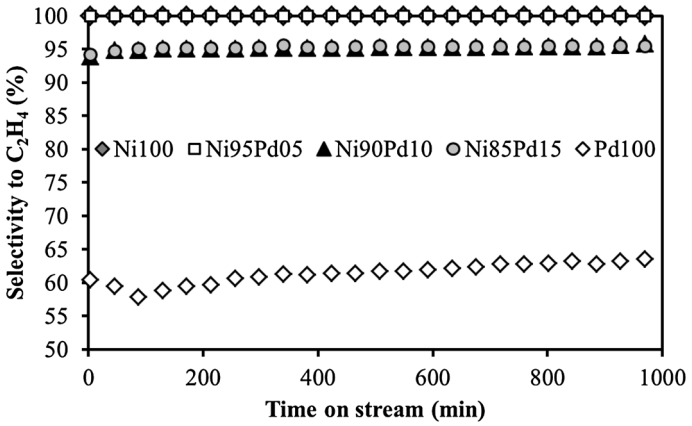

Fig. 3 Time on stream behavior. Selectivity to C_2H_4 in hydrodechlorination of 1,2-DCA

Table 2 Estimated particle sizes and dispersion for Ni–Pd catalysts, from XRD measurements

Catalyst	Particle size estimated from SEM (nm)	Particle size estimated from XRD (nm)[a]	Dispersion (%)[b]
Ni100	n.m.[c]	31	3.0
Ni95Pd05	15–20	17	6.0
Ni90Pd10	7–12	18	5.5
Ni85Pd15	7–13	20	5.0
Pd100	n.m.[c]	2	56.0

[a] Average Ni diameter based on (1 1 1) XRD line broadening

[b] Measured from XRD results

[c] Not measured

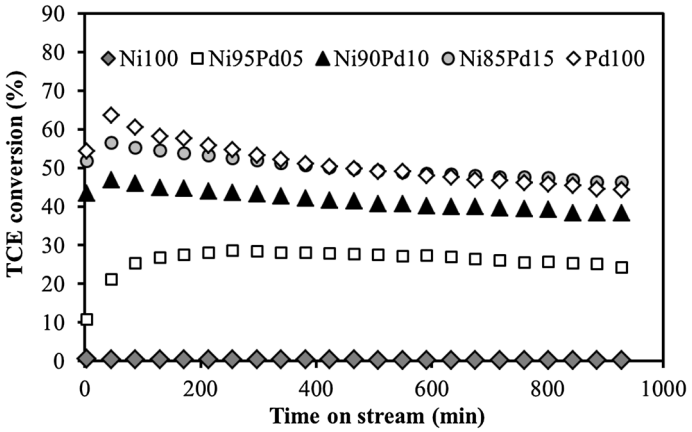

Fig. 4 Changes of conversion as a function of time on stream in HDC of TCE over Pd–Ni catalysts

Table 3 Results of TCE hydrodechlorination at 503 K (stationary state)

Catalyst	Selectivity (%)						Conversion (%)
	C_2H_4	C_3H_6	C_3H_3Cl	CH_2Cl_2	$CHCl_3$	Other products[a]	
Ni100	32.3	21.5	–	44.3	–	1.9	0.3
Ni95Pd05	29.7	2.6	2.7	12.2	38.9	13.9	25.2
Ni90Pd10	35.2	1.4	4.5	9.2	34.4	15.3	38.8
Ni85Pd15	36.0	0.7	5.4	7.2	35.6	15.1	47.0
Pd100	59.3	0.4	7.1	12.0	–	21.2	45.3

[a] Other products, e.g. C_2H_6, 1,1-dichloroethane, 1,1-dichloroethene

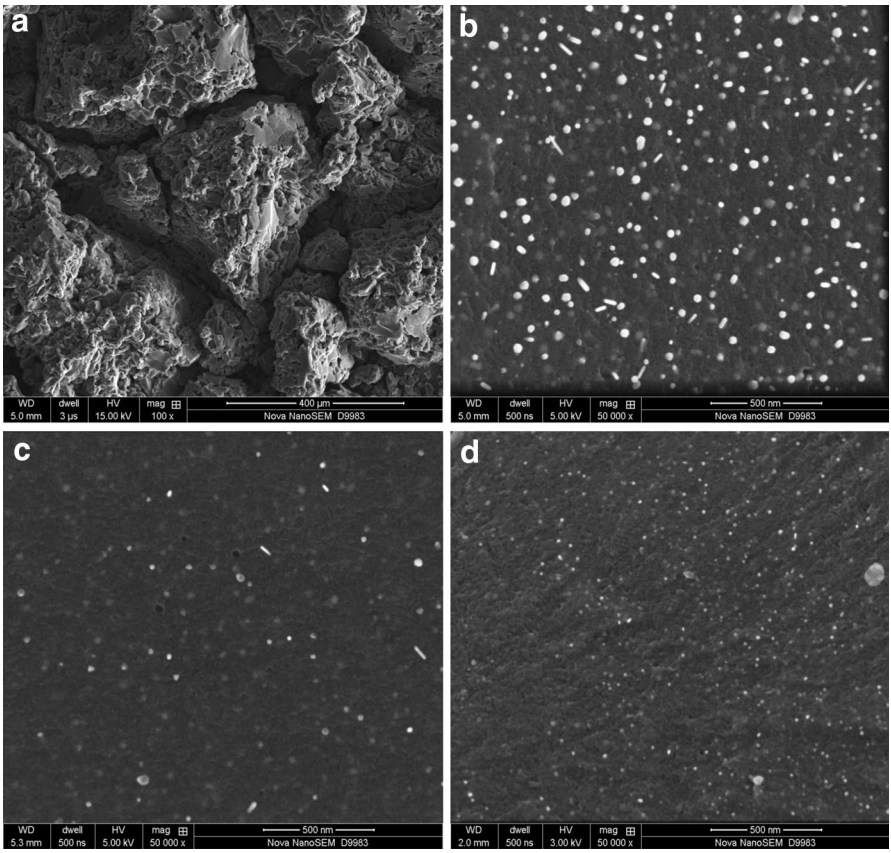

Fig. 5 SEM images: **a** Norit CNR115, and catalysts after reduction: **b** Ni95Pd05, **c** Ni90Pd10, **d** Ni85Pd15

It is worth noting here that there are few reports of catalytic conversion of TCE in the gas phase at relatively low reaction temperature −503 K. HDC of TCE has usually been performed in the temperature range 373–573 K [31], although good results have been obtained at higher temperatures [31, 32]. Meshesha et al. [33]

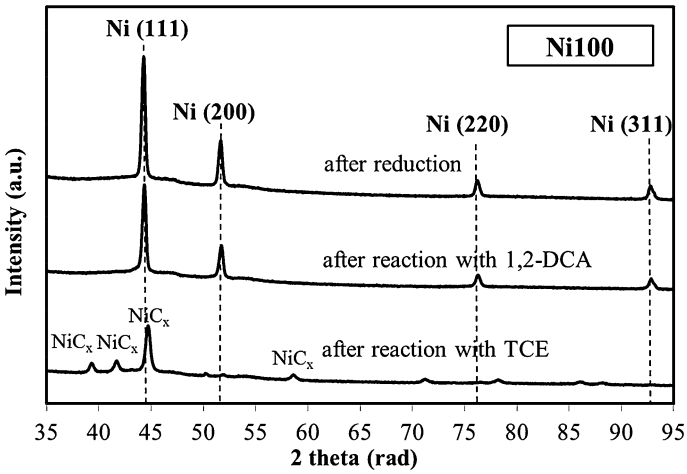

Fig. 6 XRD profiles of Norit CNR115-supported Ni100 after reduction and after hydrodechlorination of 1,2-dichloroethane and 1,1,2-trichloroethene

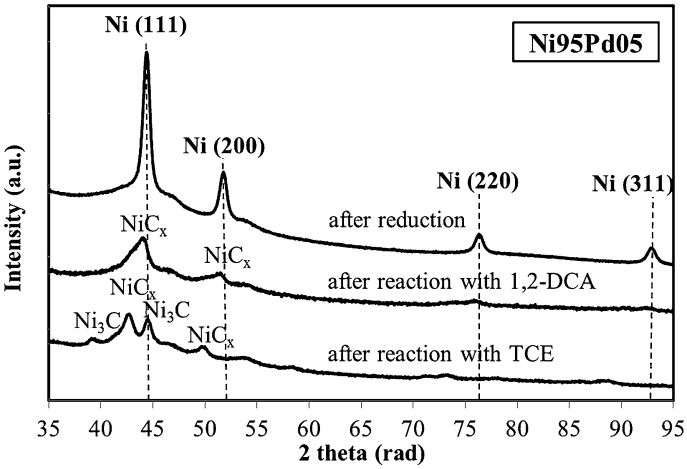

Fig. 7 XRD profiles of Norit CNR115-supported Ni95Pd05 after reduction and after hydrodechlorination of 1,2-dichloroethane and 1,1,2-trichloroethene

reported results for HDC of TCE at 573 K. During reaction for 270 min over Pd/NiMgAl mixed oxide, strong deactivation was observed, and the maximum selectivity of NiMgAl for ethylene was 55 %. Cu-hydrotalcite-derived catalysts [34] and Pt/CeO_2 [35] have very high activity at 573 K. At 473 K conversion by 0.2 $\%Pt/CeO_2$ was approximately 5 %, and ethylene and ethane were obtained as the main products. Therefore, in view of these literature data, our results obtained for HDC of trichloroethene at a relatively low reaction temperature are rather satisfactory. During reaction for $\sim$17 h we did not observe deactivation of Ni95Pd05 and Ni90Pd10. Slight deactivation of Pd100 and Ni85Pd100 was

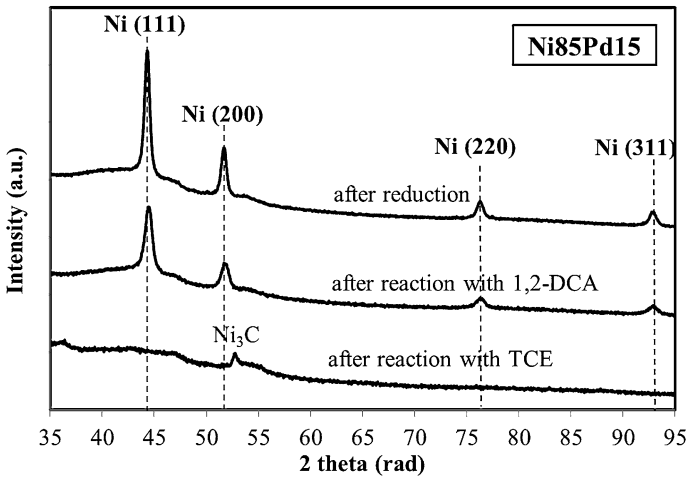

Fig. 8 XRD profiles of Norit CNR115-supported Ni85Pd15 after reduction and after hydrodechlorination of 1,2-dichloroethane and 1,1,2-trichloroethene

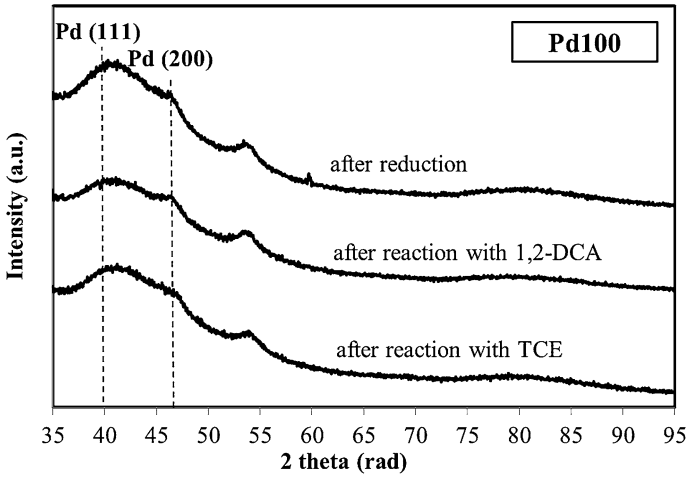

Fig. 9 XRD profiles of Norit CNR115-supported Pd100 after reduction and after hydrodechlorination of 1,2-dichloroethane and 1,1,2-trichloroethene

observed, however (Fig. 4); this could be because of palladium segregation to the surface and/or formation of carbon-containing deposits on active metal species during the HDC process.

X-ray diffraction and scanning electron microscopy measurements

XRD measurements were performed for catalysts after reduction and after HDC of 1,2-DCA and TCE. The particle sizes and metal dispersion for catalysts after

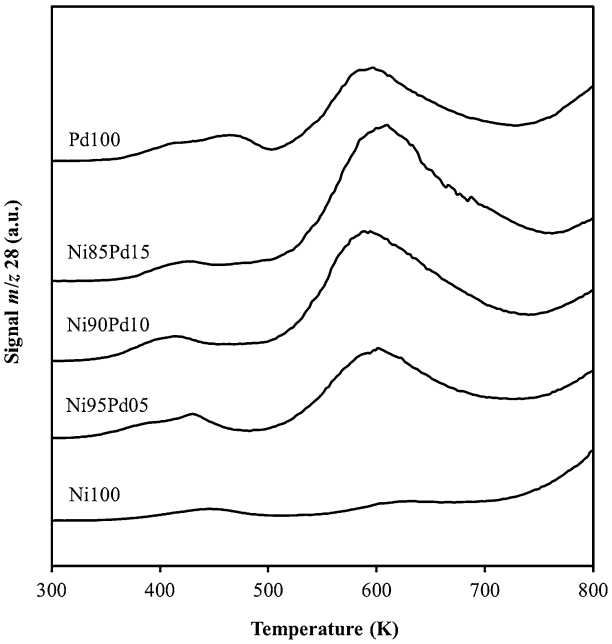

Fig. 10 TPH profiles of post-reaction deposition of C_2H_x (m/z 28) on Ni–Pd catalysts after hydrodechlorination of 1,2-dichloroethane

reduction were estimated from XRD profiles (Table 2) and SEM images (Fig. 5). Metal particles size obtained by use of SEM and XRD are not fully compatible. In general, SEM measurements resulted in smaller particle sizes than those estimated by use of XRD (Table 2).

XRD spectra for Ni100, Ni95Pd05, Ni85Pd15, and Pd100 are shown in Figs. 6, 7, 8 and 9, respectively. Comparison of the XRD profiles of the reduced and spent catalysts showed that carbiding occurred during reaction with 1,2-DCA and TCE. Formation of NiC_x solution (fcc phase) and Ni_3C (hcp phase) were observed (Figs. 6, 7 and 8). This was much more apparent for the catalysts after HDC of TCE (presence of hcp Ni_3C reflections) than of 1,2-DCA (presence of the fcc phase of NiC_x solution only), in agreement with the literature [10]. This phenomenon could be explained by higher TCE conversion (Fig. 4), although the presence of the double bond (C=C) in the molecular structure of TCE could also be of crucial importance. The presence of Ni_3C was usually observed in nickel samples subjected to such typical carbiding agents as ethene and other unsaturated hydrocarbons [22, 36]. XRD results (Figs. 6, 7 and 8) confirmed that 1,1,2-trichloroethene and/or HDC of TCE products are also efficient carbiding agents. Our results are in agreement with those obtained for Sibunit carbon-supported and alumina-supported nickel catalysts in HDC of 1,2-DCA, in which transformation of nickel to fcc NiC_x solution and/or even to the hcp Ni_3C carbide phase were observed [22, 26, 37]. This phenomenon strongly affected product distribution in HDC of 1,2-DCA [22].

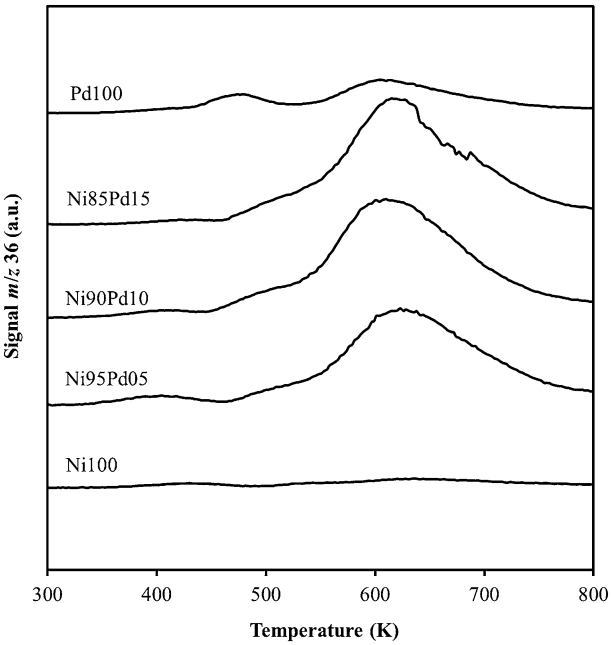

Fig. 11 TPH profiles of post-reaction deposition of HCl (*m*/*z* 36) on Ni–Pd catalysts after hydrodechlorination of 1,2-dichloroethane

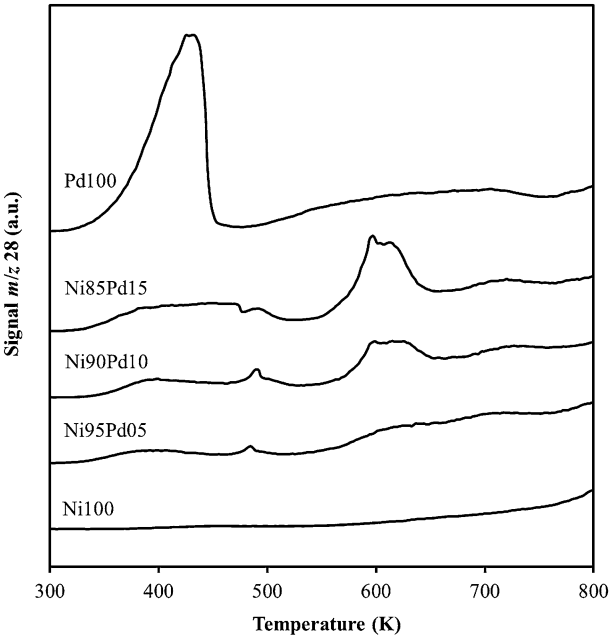

Fig. 12 TPH of post-reaction deposition of C_2H_x (*m*/*z* 28) on Ni–Pd catalysts after hydrodechlorination of 1,1,2-trichloroethene

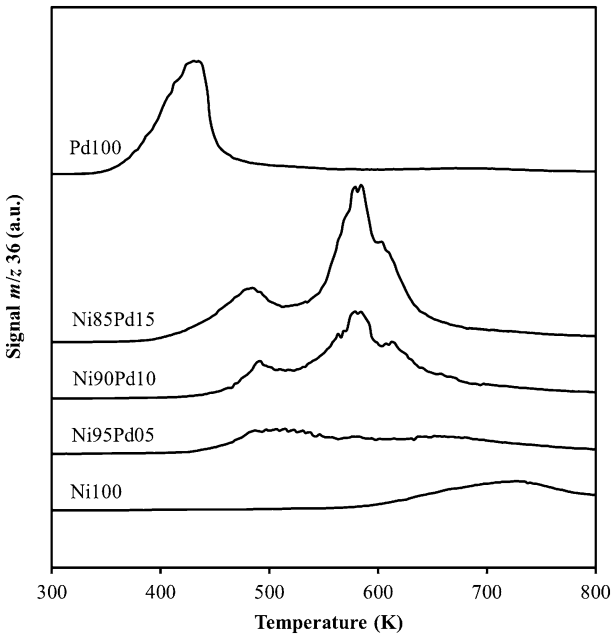

Fig. 13 TPH profiles of post-reaction deposition of HCl (*m*/*z* 36) on Ni–Pd catalysts after hydrodechlorination of 1,1,2-trichloroethene

Selectivity for ethylene decreased at the expense of increasing selectivity for vinyl chloride, in contrast with results obtained from catalytic conversion of 1,2-DCA and TCE on Norit-supported Pd–Ni catalysts. As in previous studies [26], we could not exclude transformation of Pd100 to PdC_x solution; the very high dispersion of Pd made identification of the PdC_x form impossible, however (Fig. 9). Nevertheless, palladium carbiding does not substantially affect the catalytic behavior of Pd100 or this phase variation occurs at an initial stage of the reaction.

Temperature-programmed hydrogenation measurements

TPH measurements showed that carbonaceous species were deposited on the Ni–Pd catalysts during HDC of 1,2-DCA (Figs. 10, 11) and TCE (Figs. 12, 13); this resulted in blocking of the active metal sites. Deposits containing chlorine were also observed after HDC of 1,2-DCA. A rather high temperature (600 K) was needed for hydrogenation of carbon and chlorine-containing species, suggesting strong interaction of these deposits with the surfaces of the catalysts.

Conclusions

- Active carbon (Norit)-supported Ni–Pd catalysts are active and stable in HDC of 1,2-DCA and TCE at a relatively low reaction temperature (503 K).

- Very high selectivity ($\sim$100 %) for the desired reaction product, ethene, was observed in HDC of 1,2-DCA. The main products from HDC of TCE were hydrocarbons (C_2H_4, C_2H_6, C_3H_8).
- Addition of palladium to the nickel resulted in a substantial increase in the activity of the catalysts.
- TPH measurements showed that carbon and chlorine-containing species were deposited on the catalysts during reaction with 1,2-DCA and TCE.
- During HDC of 1,2-DCA and TCE, the carbon from substrates permeated the metal phase, which led to formation of the fcc NiC_x phase and the hcp carbide Ni_3C phase.

Acknowledgments This work was funded by the National Science Centre in Poland (Research Project SONATA based on decision DEC-2011/03/D/ST5/05516).

References

1. L.H. Lash, W.A. Chiu, K.Z. Guyton, I. Rusyn, Mutat. Res. Rev. Mutat. Res. (2014). doi:10.1016/j.mrrev.2014.04.003
2. I. Rusyn, W.A. Chiu, L.H. Lash, H. Kromhout, J. Hansen, K.Z. Guyton, Pharmacol. Ther. **141**, 55 (2014)
3. N. Guha, D. Loomis, Y. Grosse, B. Lauby-Secretan, F. El Ghissassi, V. Bouvard, L. Benbrahim-Tallaa, R. Baan, H. Mattock, K. Straif, Lancet Oncol. **13**, 1192 (2012)
4. M. Martin-Martinez, L.M. Gómez-Sainero, M.A. Alvarez-Montero, J. Bedia, J.J. Rodriguez, Appl. Catal. B **132–133**, 256 (2013)
5. J. Bedia, L.M. Gómez-Sainero, J.M. Grau, M. Busto, M. Martin-Martinez, J.J. Rodriguez, J. Catal. **294**, 207 (2012)
6. E. Diaz, A.F. Mohedano, J.A. Casas, L. Calvo, M.A. Gilarranz, J.J. Rodriguez, Catal. Today (2014). doi:10.1016/j.cattod.2014.03.052
7. L. Calvo, M.A. Gilarranz, J.A. Casas, A.F. Mohedano, J.J. Rodriguez, Chem. Eng. J. **163**, 112 (2010)
8. S. Gryglewicz, W. Piechocki, Chemosphere **83**, 334 (2011)
9. Y. Xu, J. Ma, Y. Xu, H. Li, H. Li, P. Li, X. Zhou, Appl. Catal. A **413–414**, 350 (2012)
10. V. Simagina, V. Likholobov, G. Bergeret, M.T. Gimenez, A. Renouprez, Appl. Catal. B **40**, 293 (2003)
11. Y. Wang, J. Wang, G. Fan, F. Li, Catal. Commun. **19**, 56 (2012)
12. R. Baran, I.I. Kamińska, A. Śrębowata, S. Dzwigaj, Microporous Mesoporous Mater. **169**, 120 (2013)
13. J.A. Cecilia, I. Jiménez-Morales, A. Infantes-Molina, E. Rodríguez-Castellóna, A. Jiménez-Lópeza, J. Mol. Catal. A **268–269**, 78 (2013)
14. N.E. Kavalerskaya, E.S. Lokteva, T.N. Rostovshchikova, E.V. Golubina, K.I. Maslakov, Kinet. Catal. **54**, 597 (2013)
15. R. Baran, A. Śrębowata, I.I. Kamińska, D. Łomot, S. Dzwigaj, Microporous Mesoporous Meter. **180**, 209 (2013)
16. A. Śrębowata, R. Baran, D. Łomot, D. Lisovytskiy, T. Onfroy, S. Dzwigaj, Appl. Catal. B **147**, 208 (2014)
17. N. Wu, W. Zhang, B. Li, C. Han, Microporous Mesoporous Mater. **185**, 130 (2014)
18. M. Lan, G. Fan, Y. Wang, L. Yang, F. Li, J. Mater. Chem. A **2**, 14682 (2014)

19. S.L. Pirard, J.G. Mahy, J.P. Pirard, B. Heinrichs, L. Raskinet, S.D. Lambert, Microporous Mesoporous Meter. (2014). doi:10.1016/j.micromeso.2014.08.015
20. A. Śrębowata, R. Baran, D. Lisovytskiy, I.I. Kamińska, S. Dzwigaj, Catal. Commun. **57**, 107 (2014)
21. A. Śrębowata, W. Juszczyk, Z. Kaszkur, J.W. Sobczak, L. Kępiński, Z. Karpiński, Appl. Catal. A **319**, 181 (2007)
22. R.R. De Leede, E.G.J. Staal, M. Rodgers, W.M.T.M. Reimerink-Schats, American patent, US 8759253, 19 July 2008
23. N.S. Babu, N. Lingaiah, P.S. Sai Prasad, Appl. Catal. B **111–112**, 309 (2012)
24. A. Tanksale, J.N. Beltramini, J.A. Dumesic, G.Q. Lu, J. Catal. **258**, 366 (2008)
25. Y. Mukainakano, B. Li, Sh Kado, T. Miyazawa, K. Okumura, T. Miyao, Sh Naito, K. Kunimori, K. Tomishige, Appl. Catal. A **318**, 252 (2007)
26. A. Śrębowata, W. Juszczyk, Z. Kaszkur, Z. Karpiński, Catal. Today **124**, 28 (2007)
27. N. Job, B. Heinrichs, F. Ferauche, F. Noville, J. Marien, J.P. Pirard, Catal. Today **102–103**, 234 (2005)
28. S. Lambert, F. Ferauche, A. Brasseur, J.P. Pirard, B. Heinrichs, Catal. Today **100**, 283 (2005)
29. Y. Yang, C. Ochoa-Hernández, V.A. de la Peña O'Shea, P. Pizarro, J.M. Coronado, D.P. Serrano, Appl. Catal. B **145**, 91 (2014)
30. E. Diaz, A.F. Mohedano, J.A. Casas, L. Calvo, M.A. Gilarranz, J.J. Rodriguez, Appl. Catal. B **106**, 469 (2011)
31. L. Bonneviot, D. Olivier, M. Che, J. Mol. Catal. **21**, 415 (1983)
32. C.P. Heveling, M. Nicolaides, S. Scurrell, J. Chem. Soc., Chem. Commun. **2**, 126 (1991)
33. B.T. Meshesha, N. Barrabés, K. Föttinger, R.J. Chimentão, J. Llorca, F. Medina, G. Rupprechter, J.E. Sueiras, Appl. Catal. B **117–118**, 236 (2012)
34. N. Barrabes, D. Cornado, K. Foettinger, A. Dafinov, J. Llorca, F. Medina, G. Rupprechter, J. Catal. **263**, 239 (2009)
35. N. Barrabes, K. Fottinger, A. Dafinov, F. Medina, G. Rupprechter, J. Llorca, J.E. Sueiras, Appl. Catal. B **87**, 84 (2009)
36. M. Bououdina, D. Grant, G. Walker, Carbon **43**, 1286 (2005)
37. A. Śrębowata, I. Stefanowicz-Pięta, W. Juszczyk, Z. Karpiński, Pol. J. Chem. **81**, 152 (2007)